

ON THE EFFECT OF UNSTIRRED LAYERS ON K^+ -ACTIVATED ELECTROGENIC Na^+ PUMPING IN CARDIAC PURKINJE STRANDS

HELGE H. RASMUSSEN,* DAVID J. MOGUL*‡, AND ROBERT E. TENEICK§

*The Reingold ECG Center (Division of Cardiology, Department of Medicine), ‡the Department of Electrical Engineering and Computer Science, and §the Department of Pharmacology, Northwestern University, Chicago, Illinois 60611

ABSTRACT Many studies of electrogenic Na^+ pumping in Purkinje strands have involved intracellular Na^+ loading by exposure to 0 mM K^+ , followed by reexposure to K^+ . For sheep Purkinje strands the K^+ concentration for half-maximal stimulation ($K_{0.5}$) in such studies is higher than $K_{0.5}$ of canine Purkinje strands. A model was developed to determine if gradients in the K^+ concentration of extracellular fluid layers during enhanced pump activity can account for the discrepancy. Pump activity was assumed linearly dependent on $[Na^+]_i$ and dependent on $[K^+]_o$, according to Michaelis-Menten kinetics. The model simulated diffusion of K^+ across unstirred layers and both depletion and accumulation of K^+ in extracellular clefts of Purkinje strands during changes in the K^+ concentration of the tissue bath. Errors in estimates of $K_{0.5}$ occurred when delay in achieving a steady state extracellular K^+ concentration was simulated. The simulations suggested that a linear relationship between pump current and intracellular Na^+ , a monoexponential decay of pump current, independence of the rate constants for the current decay on the initial Na^+ load and holding potential, and apparent Michaelis-Menten K^+ kinetics is not sufficient evidence against pump-induced interstitial K^+ depletion having introduced errors in determination of $K_{0.5}$. It is concluded that interstitial K^+ depletion may account for the difference between determinations of $K_{0.5}$ in sheep and canine Purkinje strands.

INTRODUCTION

It is generally accepted that the sarcolemmal Na^+ -pump activity exhibits a saturable dependence on extracellular K^+ . However, important quantitative details are not well resolved. Some studies reported that the K^+ concentration at which the Na^+ pump is half maximally activated ($K_{0.5}$) is 1–1.5 mM, while others reported that $K_{0.5}$ is much higher (see Gadsby, 1984, for a review). The higher values were determined from studies of pump rate in Na^+ -loaded sheep Purkinje strands. Sodium loading was induced by exposure of the tissue to K^+ -free superfusate and pump rate was assessed on reexposure to different concentrations of K^+ (or Rb^+). The lower values for $K_{0.5}$ were determined in similar experiments on canine Purkinje strands (Gadsby and Cranefield, 1979; Gadsby, 1980) or in experiments on sheep Purkinje strands involving measurement of intracellular Na^+ ($[Na^+]_i$) during exposure to different K^+ (or Rb^+) concentrations under steady state conditions (Eisner et al., 1981b; Glitsch et al., 1981).

It has been suggested that the large $K_{0.5}$ of Na^+ -loaded sheep Purkinje strands may arise because the K^+ concentration in narrow extracellular clefts ($[K^+]_o$) is lower than

the K^+ concentration in the bulk phase of the solution ($[K^+]_b$) when pump activity is enhanced. However, it has also been speculated (Eisner and Lederer, 1980; Eisner et al., 1981b; Cohen et al., 1984) that experimental findings such as a linear relationship between $[Na^+]_i$ and pump current, a monoexponential decay of the current and the rate constants for this decay being independent of Na^+ load and holding potential (E_m) provide experimental evidence against substantial interstitial depletion of activator cation.

Cohen et al. (1984) provided an alternative explanation by demonstrating that saturation of the intracellular Na^+ binding site could account for at least part of the discrepancy between $K_{0.5}$ determined under kinetic or steady state conditions in sheep Purkinje strands. However, saturability of the Na^+ site cannot easily explain the difference between kinetic estimates of $K_{0.5}$ in sheep and in canine Purkinje strands. Therefore, we have used a theoretical model to evaluate the experimental findings that have been suggested to be evidence against interstitial depletion. These findings could be reproduced even when depletion was simulated. However, $K_{0.5}$ was overestimated when the dependence of pump currents on $[K^+]_b$ was analyzed with methods similar to those used for experimental recordings. It is concluded that interstitial K^+ depletion can at least partly account for the discrepancies between reported values for $K_{0.5}$.

Send reprint requests to Robert E. TenEick, c/o Department of Pharmacology, Northwestern University, Chicago, IL 60611.

DESCRIPTION OF MODEL

Upon reexposure to K^+ of a Na^+ -loaded Purkinje strand, the K^+ ions must equilibrate throughout the extracellular spaces before recorded currents are representative of Na^+ -pump activity at a given $[K^+]_b$. Equilibration is slowed by unstirred layers of solution adjacent to and within the connective tissue surrounding the fiber bundles. In the model, extracellular equilibration is determined by a time constant for diffusion (τ_{ex}) and the concentration gradient

$$\frac{d[K^+]_o}{dt} = \frac{[K^+]_b - [K^+]_o}{\tau_{ex}} \quad (1)$$

Uptake of K^+ via the Na^+ pump and efflux via K^+ channels may affect $[K^+]_o$ in parts of the unstirred layers corresponding to narrow extracellular clefts. We therefore modified Eq. 1. In this modification it is assumed that passive efflux of K^+ is insensitive to changes in $[K^+]_o$, an assumption that seems reasonable because K^+ -activated Na^+ pumping usually is studied using solutions that render K^+ conductance insensitive to changes in $[K^+]_o$ or, alternatively, cations other than K^+ are used for pump activation. It is also assumed that the Na/K exchange ratio is 3:2. The modified equation is

$$\frac{d[K^+]_o}{dt} = \frac{[K^+]_b - [K^+]_o}{\tau_{ex}} - \frac{2 \Delta I_p S_{cell}}{F V_{cleft}} + \frac{g_K (E_m - E_K) S_{cell}}{F V_{cleft}} \quad (2)$$

where F is Faraday's constant, ΔI_p is the current density resulting from pumping of the Na^+ load, and S_{cell}/V_{cleft} is the ratio of cell surface area to interstitial cleft volume for sheep Purkinje strands ($170 \mu m^{-1}$; obtained from Mobley and Page, 1972), g_K is the K^+ conductance, and E_K is the equilibrium potential for K^+ . E_K is calculated assuming that the intracellular K^+ concentration ($[K^+]_i = 150 \text{ mM}$)

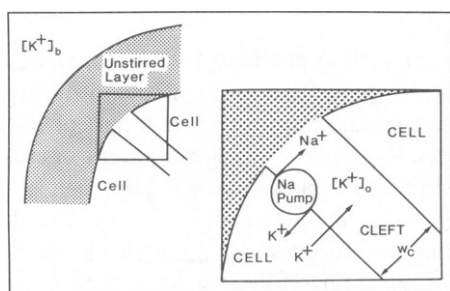


FIGURE 1 Diagram of model. The patch of membrane modeled is assumed juxtaposed to a narrow extracellular cleft of a constant width (w_c). Na^+ -pump function of the patch is responsive only to the K^+ concentration of the cleft ($[K^+]_o$). The cleft if located adjacent to a much larger compartment of unstirred layers. $[K^+]_o$ is determined by the K^+ concentration in the bulk phase ($[K^+]_b$), the time constant for diffusion across the unstirred layers (τ_{ex}), uptake of K^+ by the Na^+ pump and passive transmembrane K^+ efflux. The K^+ concentration in the large compartment of unstirred layers is unaffected by transmembrane transport.

is constant, an assumption that results in only small errors in the simulations to be presented because of the logarithmic relationship between $[K^+]_i$ and E_K . Equations of this general form are based on simplifying geometrical assumptions. In essence they describe the time course of $[K^+]_o$ in a narrow half-cleft in series with a much larger compartment of unstirred solution (Coulombe and Coraboeuf, 1983). See Fig. 1 for diagrammatic representation of the model.

Such sharp distinction between the two compartments is artificial in view of the complex architecture of Purkinje strands. As a consequence of the geometric simplicity of the model, the weights of the second and third terms on the right side of Eq. 2, relative to what they should be for geometrically more accurate model, are probably not appropriate. To allow for these uncertainties and to be able to adjust for the wide range of values reported for S_{cell}/V_{cleft} (Hellam and Studt, 1974; Eisenberg and Cohen, 1983) Eq. 2 is modified with the dimensionless factor Z

$$\frac{d[K^+]_o}{dt} = \frac{[K^+]_b - [K^+]_o}{\tau_{ex}} - \frac{2 \Delta I_p S_{cell} Z}{F V_{cleft}} + \frac{g_K (E_m - E_K) S_{cell} Z}{F V_{cleft}} \quad (3)$$

For a given τ_{ex} , Z was adjusted to obtain currents that mimic experimental records. Since S_{cell}/V_{cleft} is almost equal to $2/w_c$, where w_c is mean-cleft width (Hellam and Studt, 1974), changes in w_c can be emulated by changing S_{cell}/V_{cleft} . Changes in S_{cell}/V_{cleft} , in turn, are equivalent to changes in Z (Eq. 3). Therefore, effects of changes in w_c can be examined by varying Z .

After elevation by exposure to 0 mM K^+ , when K^+ is reintroduced, intracellular Na^+ returns to steady state ($[Na^+]_{i-K_0}$). If background Na^+ influx is independent of $[K^+]_o$, $[Na^+]_{i-K_0}$ is determined by $[K^+]_o$ according to Michaelis-Menten kinetics (Cohen et al., 1984)

$$\frac{[K^+]_o}{K_{0.5} + [K^+]_o} [Na^+]_{i-K_0} = \text{constant} \quad (4)$$

We estimated the constant at 4.8 (Table I; Cohen et al., 1984).

For a total intracellular Na^+ concentration ($[Na^+]_i$) at a given $[K^+]_o$ the Na^+ load ($[\Delta Na^+]_i$) is defined by

$$[\Delta Na^+]_i = [Na^+]_i - [Na^+]_{i-K_0} \quad (5)$$

The Na^+ load in the model is thus defined by $[Na^+]_i$ and $[K^+]_o$. Since $[K^+]_o$ changes with time (Eq. 3) the fraction of $[Na^+]_i$ perceived as a load is also changing (Eq. 4 and 5).

It is apparent from Eq. 4 that $[Na^+]_{i-K_0}$ is large for small values of $[K^+]_o$, and may therefore exceed $[Na^+]_i$. When this occurred it was made equal to $[Na^+]_i$. This prevented mathematical instability and restricted simulations to conditions of Na^+ loading. For starting conditions, $[K^+]_o$ was set at a very small but nonzero value (to avoid an infinite value of E_K in Eq. 3). Subsequently, the model

calculated $[K^+]_o$ according to Eq. 3 with ΔI_p equal to zero until $[Na^+]_{i-K_0}$, calculated according to Eq. 4, became smaller than $[Na^+]_i$. For each subsequent time step, $[Na^+]_{i-K_0}$ derived from Eq. 4 was used to calculate $[\Delta Na^+]_i$ using Eq. 5. The pump-current density resulting from the net load was assumed to follow nonsaturable Na^+ kinetics

$$\frac{d[\Delta Na^+]_i(\text{pump})}{dt} = -k[\Delta Na^+]_i \quad (6)$$

$$= \frac{3 \Delta I_p S_{\text{cell}}}{FV_{\text{cell}}}, \quad (7)$$

where $S_{\text{cell}}/V_{\text{cell}}$ is the cell surface area to volume ratio (Mobley and Page, 1972) and the first-order rate constant, k , is assumed to be $[Na^+]_i$ -insensitive but dependent upon $[K^+]_o$ according to

$$k = \frac{k_{\text{max}} [K^+]_o}{[K^+]_o + K_{0.5}}, \quad (8)$$

where k_{max} is the rate constant as $[K^+]_o$ goes to infinity. In accordance with Cohen et al. (1984) k_{max} was chosen to give a k of $1/75 \text{ s}^{-1}$ in 4 mM $[K^+]_o$ when $K_{0.5}$ is equal to 1 mM. Since $[K^+]_o$ changes with time according to Eq 3, k also changes. It was assumed that the Na^+ pump is the only efflux route for Na^+ and that background Na^+ influx is independent of any other efflux mechanisms and $[K^+]_o$, assumptions also necessary for analysis of experimentally obtained data (Cohen et al., 1984). Eqs. 7 and 8 were used to solve for ΔI_p , which was then inserted into Eq. 3 for the next time increment. Solutions of Eqs. 3 and 6 were obtained using the fourth-order Runge-Kutta algorithm (Gerald, 1980). The model was programmed in Pascal (MS-Pascal; Microsoft Corp., Bellevue, WA) and run on a microcomputer (model Z-150; Zenith Data Systems, Chicago, IL).

RESULTS

All simulations were performed assuming that true $K_{0.5}$ is 1 mM. Effects of delays in diffusion of K^+ were examined by varying the values of τ_{ex} , and effects of pump-induced alterations in $[K^+]_o$ in extracellular clefts were examined by varying Z (see Eq 3). Currents simulated when g_K as estimated from the literature (Glitsch et al., 1982) was inserted into Eq 3 were virtually indistinguishable from currents simulated when g_K was 0 S/cm². Therefore, except when indicated, g_K was set at 0 S/cm². Initial $[Na^+]_i$ was 20 mM unless otherwise indicated. ΔI_p increased

Effect of Delays in K^+ Equilibration on Simulated Pump Currents

Fig. 2 depicts $[K^+]_o$ and ΔI_p for two different values of τ_{ex} (2 or 30 s) on exposure of Na^+ loaded tissue to a $[K^+]_b$ of 4 mM. The effects of Na^+ pumping on $[K^+]_o$ in extracellular clefts was assumed to be negligible ($Z = 0$). ΔI_p increased

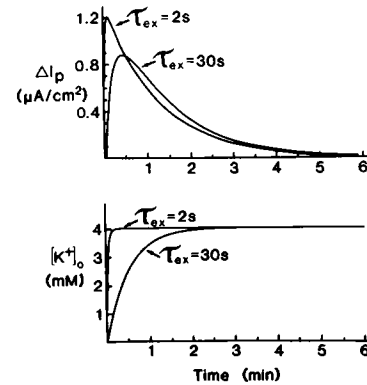


FIGURE 2 Effect of varying τ_{ex} on simulated pump currents. The top depicts ΔI_p for simulations with a τ_{ex} of 2 or 30 s. The bottom depicts corresponding time courses of $[K^+]_o$. $[K^+]_o$ was assumed to be unaffected by Na^+ -pump activity ($Z = 0$) and $[K^+]_b$ was 4 mM. Peak ΔI_p for τ_{ex} going toward 0 was $1.3 \mu\text{A}/\text{cm}^2$ (data not shown).

slowly to a delayed peak when τ_{ex} was 30 s, results comparable to experimental pump currents from sheep Purkinje strands (Eisner and Lederer, 1980). In addition, peak amplitude of ΔI_p was reduced for a τ_{ex} of 30 s suggesting that the amplitude of pump current may not be an appropriate index of pump activity at a given $[K^+]_b$ when K^+ equilibration is delayed.

Fig. 3 demonstrates how interstitial K^+ depletion can alter the time courses of $[K^+]_o$ and ΔI_p . τ_{ex} for both of the depicted simulations is 2 s, and Z is 0 or 0.0085. $[K^+]_b$ is 4 mM. The time course of $[K^+]_o$ is markedly altered by Na^+ -pump activity for $Z = 0.0085$. The amplitude of the pump current, however, is only slightly reduced (top). Fitting of the time course of ΔI_p to a monoexponential function (see below) demonstrates that the rate constant is also slightly reduced (from $1/75 \text{ s}^{-1}$ to $1/80 \text{ s}^{-1}$). Similar simulations were performed with a $[K^+]_b$ of 1 rather than 4 mM. τ_{ex} and Z were assigned the same values ($\tau_{\text{ex}} = 2 \text{ s}$, $Z = 0.0085$) as used for the simulations for a $[K^+]_b$ of 4

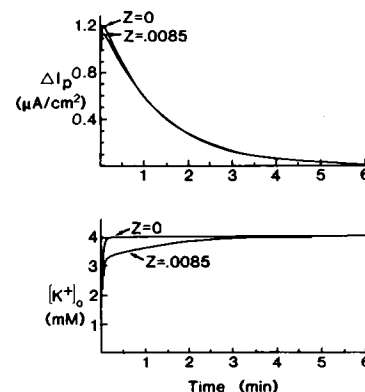


FIGURE 3 Effect of interstitial K^+ depletion on simulated pump current for a $[K^+]_b$ of 4 mM. The top depicts ΔI_p for simulations with ($Z = 0.0085$) or without ($Z = 0$) pump-induced interstitial K^+ depletion. The bottom depicts the corresponding time courses of $[K^+]_o$. τ_{ex} was 2 s for both simulations.

mM. The results are depicted in Fig. 4. The interstitial K^+ depletion causes a reduction in the amplitude of ΔI_p , and fitting the decay of ΔI_p to a monoexponential function demonstrates that the rate constant is also reduced (from $1/120$ to $1/171 \text{ s}^{-1}$).

A monoexponential decay of K^+ -activated pump current has been taken as evidence that, after a change in $[K^+]_b$, $[K^+]_o$ achieves its steady state level sufficiently fast to allow evaluation of pump currents as a function of $[K^+]_b$. In agreement with this notion it follows from Eqs. 7 and 8 that the decay of ΔI_p does not follow first-order kinetics unless $[K^+]_o$ changes rapidly upon changing $[K^+]_b$ and remains constant. The decay of ΔI_p might therefore deviate from a singly exponential when $[K^+]_o$ continues to change according to Eq. 3. To examine if such deviation occurs several semilogarithmic plots of simulated pump currents are shown in Fig. 5. $[K^+]_b$ is 1 mM (A) or 4 mM (B), and four different combinations of values for τ_{ex} and Z are used (see legend). In keeping with analysis of experimental recordings published by Eisner et al. (1981b), the first 15 s after the peak of the simulated currents were excluded from analysis. Large delays in extracellular K^+ equilibration occur in some of the simulations due to the values chosen for τ_{ex} and Z . Despite these delays, the decays of all currents appear to approximate a single exponential. However, for the same $[K^+]_b$ the rate constants determined from the plots are not identical. Interstitial K^+ depletion contributes to the delay in equilibration in two of the simulations (see legend). This causes substantial reduction in the rate of decay of pump currents when $[K^+]_b$ is 1 mM (A) while the reduction in rate of decay under the same circumstances is much less apparent when $[K^+]_b$ is 4 mM (B). However, only the simulation which assumes both that diffusion of K^+ across the unstirred layer is rapid and that $[K^+]_o$ is unaffected by pump activity ($Z = 0$) throughout the unstirred layers yields the correct rate constants. This suggests that an approximately monoexponential decay of pump currents is not sufficient evidence to indicate that

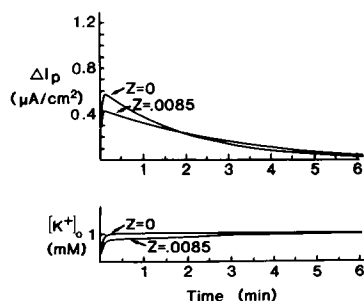


FIGURE 4 Effect of interstitial K^+ depletion on simulated pump current for a $[K^+]_b$ of 1 mM. The top depicts ΔI_p for simulations with ($Z = 0.0085$) or without ($Z = 0$) pump-induced K^+ depletion. The bottom depicts the corresponding time courses of $[K^+]_o$. τ_{ex} was 2 s for both simulations. Note that the effect of depletion on peak amplitude and rate of decay of ΔI_p is larger than the effect of depletion at the higher level of $[K^+]_b$ in the simulations depicted in Fig. 3.

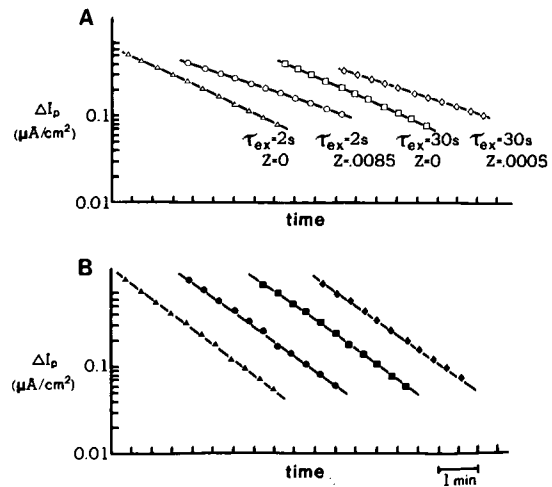


FIGURE 5 Semilogarithmic plots of pump current for a $[K^+]_b$ of 1 mM (A) or 4 mM (B). The values for τ_{ex} were 2 or 30 s. Pump-induced interstitial K^+ depletion was simulated in some of the examples by assigning Z a value of 0.0085 (for $\tau_{ex} = 2$ s) or 0.0005 (for $\tau_{ex} = 30$ s). Values for τ_{ex} and Z for the simulations are indicated in the figure. The simulated currents, plotted at 20-s intervals, are fitted with straight lines by eye. The plots are displaced with respect to each other arbitrarily along the time axis to avoid overlap. Currents are not plotted for the first 15 s after the peak. For the larger τ_{ex} (30 s) nonexponential decay was detectable during the first 15 s after the peak (data not shown).

equilibration of K^+ is unaffected by Na^+ -pump activity. Incorrect rate constants, particularly at low $[K^+]_b$, may be obtained when equilibration is delayed despite apparently monoexponential decays of the pump current.

Relationship Between $[Na^+]_i$ and Pump Current

The relationship between intracellular Na^+ activity and pump current during Rb^+ -activated Na^+ pumping is approximately linear in sheep Purkinje strands (Eisner et al., 1981b). It was suggested that such a linear relationship would not be expected if substantial pump-induced interstitial Rb^+ depletion occurred. We performed simulations to examine the relationship between $[Na^+]_i$ and ΔI_p predicted when diffusion across the unstirred layer was either rapid ($\tau_{ex} = 2$ s) or relatively slow ($\tau_{ex} = 30$ s). $[K^+]_o$ in extracellular clefts was simulated to be influenced by pump activity. Substantial delay in K^+ equilibration occurred for the values of τ_{ex} and Z chosen. As a consequence of the delay, the time course of ΔI_p was altered (see semilogarithmic plots in Fig. 5). However, the relationship between $[Na^+]_i$ and ΔI_p remained approximately linear (Fig. 6), indicating that a linear relationship is not sufficient evidence to indicate that equilibration of activator cation is rapid and unaffected by Na^+ -pump activity.

Dependence of Rate of Decay of Pump Current on Na^+ Load

The rate of decay of Rb^+ -activated pump current is virtually independent of the intracellular Na^+ load (Eisner

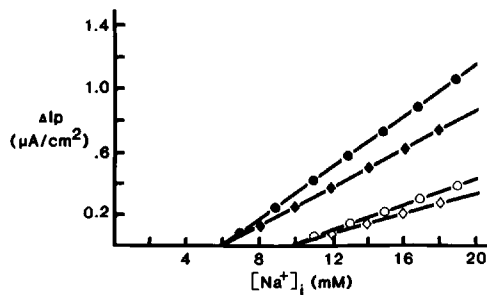


FIGURE 6 Effect of simulated interstitial K^+ depletion on the relationship between $[Na^+]_i$ and pump current. The values for τ_{ex} were 2 s (circles) or 30 s (diamonds) and $[K^+]_b$ was 1 mM (unfilled symbols) or 4 mM (filled symbols). Pump-induced K^+ depletion was simulated by assigning Z a value of 0.0085 (for $\tau_{ex} = 2$ s) or 0.0005 (for $\tau_{ex} = 30$ s). Note that the relationship between ΔI_p and $[Na^+]_i$ is approximately linear despite interstitial K^+ depletion in all simulations.

and Lederer, 1980; Eisner et al., 1981a). It was suggested that such independence would not be expected if substantial pump-induced interstitial Rb^+ depletion occurred. We performed simulations to examine this prediction. $[Na^+]_i$ at the onset of pump activation ranged from 9 to 21 mM, and it was assumed that pump activity influences $[K^+]_o$. The combinations of values chosen for τ_{ex} and Z were the same as those used in the simulations depicted in Fig. 6. To allow comparison with experimental data (Eisner et al., 1981a) $[K^+]_b$ was 10 mM and the half-time ($t_{0.5}$) was used as an index for the rate of decay of pump current. It appears from Fig. 7 that $t_{0.5}$ is essentially independent of the initial Na^+ load when τ_{ex} is 2 s, while $t_{0.5}$ decreases slightly as the degree of Na^+ loading increases when τ_{ex} is 30 s. Results obtained when time constants rather than half-times were used are similar. Experimental findings similar to the results of either simulation shown in Fig. 7 have been reported (Eisner and Lederer, 1980; Eisner et al., 1981a). This suggests that such findings do not necessarily indicate that equilibration of activator cation is rapid and unaffected by pump activity.

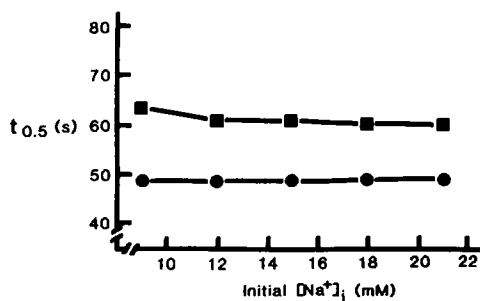


FIGURE 7 Effect of simulated interstitial K^+ depletion on the relationship between the initial $[Na^+]_i$ and half-time of decay of pump current ($t_{0.5}$). The values for τ_{ex} were 2 s (circles) or 30 s (squares) and $[K^+]_b$ was 10 mM. Pump-induced K^+ depletion was simulated by assigning Z a value of 0.0085 (for $\tau_{ex} = 2$ s) or 0.0005 (for $\tau_{ex} = 30$ s).

Effect of Delay in K^+ Equilibration on the Apparent $K_{0.5}$

The data presented in Fig. 5 suggests that the rate of decay of pump current is more sensitive to a delay in extracellular K^+ reaching a steady state when $[K^+]_b$ is low. Simulations were performed to examine how a difference in sensitivity to such delay would affect the apparent $K_{0.5}$. Results are depicted in Fig. 8. The double reciprocal plot of $[K^+]_b$ vs. rate constants for decay of pump currents was linear and a correct estimate of $K_{0.5}$ was obtained when both diffusion of K^+ across the unstirred layers was assumed to be rapid ($\tau_{ex} = 2$ s) and $[K^+]_o$ was unaffected by Na^+ -pump activity ($Z = 0$). However, $K_{0.5}$ was overestimated at 2.5 mM when interstitial K^+ depletion was simulated (Fig. 8 A). Simulations were also performed assuming that τ_{ex} was 30 s (Fig. 8 B). $K_{0.5}$ was correctly estimated when $[K^+]_o$ was unaffected by Na^+ -pump activity, whereas $K_{0.5}$ was overestimated at 2 mM when Na^+ -pump activity in the simulation affected $[K^+]_o$ ($Z = 0.0005$). The double reciprocal plots in Fig. 8 are well fit by straight lines indicating that the dependence of Na^+ -pump activity on $[K^+]_b$ appears to obey Michaelis-Menten kinetics despite delays in K^+ equilibration.

The contribution of Na^+ -pump activity to the delay in K^+ equilibration can be reduced by reducing Z (Eq. 3). Such reduction is equivalent to an increase in mean-cleft width (see Description of Model). Simulations were performed with Z reduced from the level used in Fig. 8 B (0.0005) to either 0.00025 or 0.00005. $K_{0.5}$ was overestimated (1.5 mM) when Z was 0.00025 and nearly correctly estimated (1.1 mM) when Z was 0.00005, suggesting that the width of the extracellular clefts can importantly influence estimates of $K_{0.5}$ obtained experimentally.

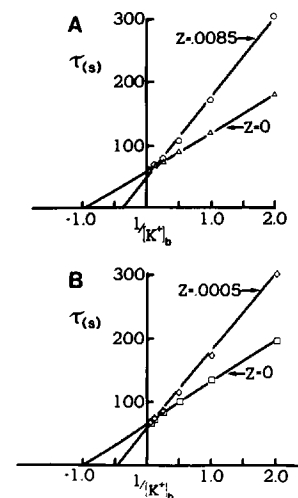


FIGURE 8 Double reciprocal plots of rate constant for decay of pump current (τ^{-1}) vs. $[K^+]_b$ from simulations with τ_{ex} of 2 s (A) or 30 s (B). The time course for $[K^+]_o$ was either independent of Na^+ -pump activity or dependent on pump activity according to the values for Z indicated in the figure.

Effect of Background K⁺ Permeability on Pump Current and K_{0.5}

In simulations presented in the preceding sections we assumed that the effect of background K⁺ permeability on [K⁺]_o is negligible under conditions used to study electrogenic Na⁺ pumping ($g_K = 0$ S/cm² in Eq 3). However, in reality background K⁺ permeability is not totally eliminated. We therefore estimated g_K from the slope conductance and clamped surface area for sheep Purkinje strands exposed to Ba²⁺ (Glitsch et al., 1982), and repeated all simulations with the derived value (10^{-6} S/cm²) inserted into Eq. 3. E_m was set at -50 mV. Results of the simulations were virtually indistinguishable from results presented in Figs. 2–7.

The effect on pump currents of changing g_K was examined at 1 and 4 mM [K⁺]_b for $\tau_{ex} = 2$ s, $Z = 0.0085$, and $E_m = -50$ mV. The simulated currents were well fit by monoexponential functions. Rate constants are depicted in the top of Fig. 9. It is apparent that background K⁺ permeability has little effect when the value of g_K is close to that estimated from experimental data (10^{-6} S/cm²) and that the rate constants are more sensitive to K⁺ permeability at 1 mM than at 4 mM [K⁺]_b. Simulations were performed to examine how this difference in sensitivity affects K_{0.5} for various levels of g_K . Background K⁺ permeability was found to have relatively little effect on K_{0.5} when g_K is approximately the value estimated from

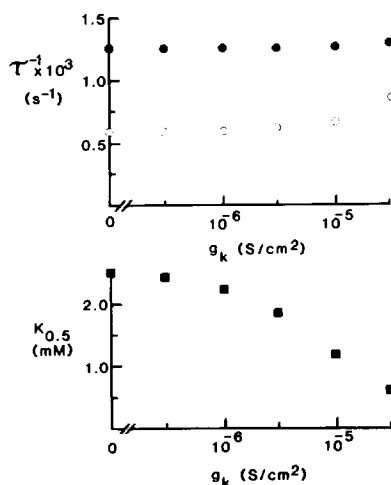


FIGURE 9 (Top) Rate constants (τ^{-1}) for decay of pump currents as a function of g_K at a [K⁺]_b of 1 mM (unfilled circles) and 4 mM (filled circles). Interstitial accumulation/depletion of K⁺ was simulated by assigning Z a value of 0.0085. E_m and τ_{ex} were -50 mV and 2 s, respectively. (Bottom) Effect of g_K on apparent K_{0.5}. Rate constants (τ^{-1}) for decay of pump currents were determined for 0.5 to 16 mM [K⁺]_b, and values for K_{0.5} were derived from double reciprocal plots of [K⁺]_b vs. τ^{-1} . E_m , τ_{ex} and Z were assigned the same values as in the upper panel. Note that K_{0.5} for a g_K of 10^{-6} S/cm² was slightly lower than K_{0.5} for a g_K of 0 S/cm² despite the similarity in rate constants at 1 and 4 mM [K⁺]_b (upper panel). The difference in K_{0.5} arose because of the effect of background K⁺ permeability on τ^{-1} for the lowest value of [K⁺]_b (0.5 mM) used to determine K_{0.5}.

experimental data. However, the apparent K⁺ sensitivity of the Na⁺ pump increased substantially for higher values of g_K (Fig. 9, bottom).

Most experimental approaches used to study K⁺-activated Na⁺ pumping have involved voltage clamping. Voltage clamping can, depending on E_m , cause interstitial depletion or accumulation of K⁺ in Purkinje strands (Baumgarten and Isenberg, 1977). Since E_m can influence [K⁺]_o, it should also influence the Na⁺-pump current if pump-induced K⁺ depletion occurs (Cohen et al., 1984). Contrary to this expectation, Eisner and Lederer (1980) and Glitsch et al. (1982) reported that the rate constants for decay of pump current in sheep Purkinje strands were independent of E_m . However, g_K , and hence the dependence of [K⁺]_o on E_m , was reduced by inclusion of Ba²⁺ in the superfusate (Glitsch et al., 1982) or by use of Cs⁺ rather than K⁺ as activator cation (Eisner and Lederer, 1980). The effect of E_m on pump currents under similar conditions was simulated by assigning g_K a value derived from the experiments using Ba²⁺ (10^{-6} S/cm²) (Glitsch et al., 1982). The values for τ_{ex} and Z were 2 s and 0.0085, respectively, and in accordance with the protocols used experimentally, a rather high [K⁺]_b (13.5 mM) was used for these simulations. The difference between any of the rate constants for decay of pump current simulated at 10-mV intervals from 0 to -80 mV was $<5.6\%$. Similar simulations were performed assigning g_K a 10-fold higher value ($g_K = 10^{-5}$ S/cm²). The differences between rate constants were $<10\%$. The voltage range for these simulations is larger than that used in published experiments (Eisner and Lederer, 1980; Glitsch et al., 1982), and the differences between the rate constants are less than the experimental errors. Therefore, an apparent absence of voltage dependence of the pump current at high concentration of activator cation cannot be used as evidence to rule out the possibility of overestimating K_{0.5} because of interstitial depletion.

K⁺ Depletion and Apparent Temperature Dependence of the Na⁺ Pump

Since electrogenic Na⁺ pumping is temperature dependent (Eisner and Lederer, 1980; Glitsch and Pusch, 1984) pump-induced interstitial K⁺ depletion should also be temperature dependent. Simulations were performed to examine the effect of depletion on the apparent temperature sensitivity of the Na⁺ pump. K_{max} in Eq. 8 was varied with temperature according to the modified Arrhenius Equation (Glitsch and Pusch, 1984) and the activation energy for the Na⁺ pump was assumed constant from 22° to 42°C. Simulations with a [K⁺]_b of 1 or 4 mM, a τ_{ex} of 2 s and values for Z of 0 or 0.0085 were performed. Pump activity in the absence of interstitial depletion followed predictions of the modified Arrhenius equation. Depletion distorted the temperature dependence, particularly at low [K⁺]_b (Fig. 10).

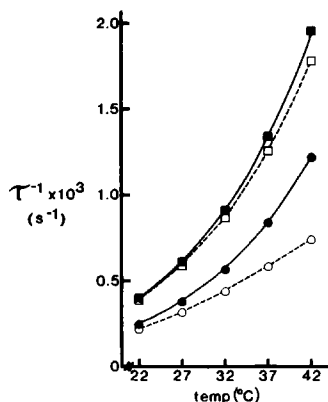


FIGURE 10 Effect of simulated interstitial K^+ depletion on the temperature dependence of the rate constant (τ^{-1}) for decay of pump current. τ_{ex} was 2 s in all simulations and $[K^+]_o$ was 4 mM (squares) or 1 mM (circles). Simulations with ($Z = 0.0085$) or without ($Z = 0$) pump-induced interstitial K^+ depletion are depicted by unfilled and filled symbols, respectively. Temperature dependence of pump activity was calculated from the modified Arrhenius equation assuming an activation energy of 15 kcal/mol.

A deviation from the expected temperature dependence has also been reported for K^+ -activated electrogenic Na^+ pumping in sheep Purkinje strands by Glitsch and Pusch (1984). A similar deviation could be simulated by our model. However, when parameters of the model were adjusted to reproduce the $K_{0.5}$ they reported, depletion had little effect at the $[K^+]_o$ used in their studies of the temperature dependence (13.5 mM). Therefore, the deviation from the expected temperature dependence in their study does not appear attributable solely to interstitial K^+ depletion.

Since the effect of K^+ depletion should be larger at higher than at lower temperatures (Fig. 10), the effect of depletion on the apparent K^+ sensitivity should be reduced by a reduction in temperature. Simulations were performed to examine this notion. Values for τ_{ex} and Z in these simulations were 2 s and 0.0085, respectively, and the experimental temperature was 27 rather than 37°C. The apparent $K_{0.5}$ at 27°C (1.6 mM) was considerably lower than $K_{0.5}$ at 37°C (2.5 mM, Fig. 8 A). Thus, the effect of temperature on the extent of interstitial K^+ depletion may cause an apparent increase in the K^+ sensitivity of Na^+ pump when temperature is decreased. Such an increase, rather than an intrinsic change in the Na^+ pump, may explain the decrease of $K_{0.5}$ reported by Glitsch and Pusch (1984) from 2.6 mM at 37°C to 2.0 mM at 20.5°C.

DISCUSSION

The Model and Its Parameters

This study examines how diffusion of K^+ across unstirred layers and accumulation/depletion of K^+ in interstitial spaces may influence K^+ -activated electrogenic Na^+ pumping. The sarcolemmal pump current density must be nonuniformly distributed, while K^+ equilibrates in the

extracellular spaces. In principle, it should be possible to model this distribution and, in turn, reconstruct the pump current for a Purkinje strand on the basis of a distributed parameter model. For strands of small diameter ($<100 \mu m$) the geometric arrangement of the myocytes may indeed allow a meaningful description of the extracellular space by distributed parameter models (Schoenberg and Fozzard, 1979). However, the sheep Purkinje strands typically used to study K^+ -activated electrogenic Na^+ pumping have been much larger. The arrangement of myocytes in such strands is very complex, and large errors may occur in the morphometric analysis of the extracellular spaces (Hellman and Studt, 1974). Therefore, it did not seem reasonable to attempt development of a distributed parameter model for this study. A lumped parameter model (see Takahashi et al., 1970 for general properties of such models) describing the pump-current density at a hypothetical representative location was used as the more reasonable alternative.

The representative patch of membrane described by the model faces an extracellular cleft of constant width. In reality, the myocyte surfaces in a Purkinje strand face extracellular spaces of a highly variable geometry including unrestricted spaces. The dimensionless factor Z was included in Eq. 3 to adjust for the inaccuracy inherent in the modeling paradigm and, in accordance with a previously published similar model (Whisler and Johnson, 1979), Z could be varied in different simulations to adjust for geometric variability of the extracellular space. The model can describe functional consequences of relative differences in mean-cleft width (Coulombe and Coraboeuf, 1983). However, for the present study, conclusions pertaining to absolute values of this parameter are not justified because of the geometric simplification.

Na^+ -pump activity was assumed linearly dependent on $[Na^+]_i$, an assumption that, for the range of $[Na^+]_i$ used in this study, is supported by experimental evidence from sheep Purkinje strands (Eisner et al., 1981b). Such first-order kinetics predicts a monoexponential decay of pump current provided K^+ equilibrates rapidly in the extracellular space. However, delays in achieving K^+ equilibration might seriously distort the time course of the current. This was indeed found to be the case, but despite the distortion, a good approximation to a monoexponential decay of simulated currents was obtained.

Effect of Delays in Interstitial K^+ Equilibration on $K_{0.5}$

The rate constants for decay of pump current for a range of $[K^+]_o$'s were used to determine an apparent $K_{0.5}$ (Fig. 8). For a τ_{ex} of 2 or 30 s a correct estimate was obtained provided $[K^+]_o$ was assumed to be unaffected by Na^+ -pump activity. Similar simulations demonstrated that $K_{0.5}$ was fairly accurately estimated for values of τ_{ex} up to 100 s (data not shown). $K_{0.5}$ was overestimated for larger values of τ_{ex} . Overestimation of $K_{0.5}$ occurred for much lower

values of τ_{ex} when it was assumed that Na^+ -pump activity influences $[\text{K}^+]_o$ in extracellular clefts, and mean-cleft width was an important determinant of the apparent $K_{0.5}$ value. These findings suggest that error in the experimental estimation of $K_{0.5}$ may develop if a large fraction of the sarcolemmal surface of a Purkinje strand faces narrow extracellular clefts. In contrast, estimates of $K_{0.5}$ should be more accurate if cell surfaces predominantly face wide extracellular spaces. Since the mean-cleft width is larger and the fraction of the myocyte surface facing the clefts is smaller for canine than for sheep Purkinje strands (Eisenberg and Cohen, 1983), this may explain why kinetic estimates of $K_{0.5}$ are severalfold lower for canine (Gadsby and Cranefield, 1979; Gadsby, 1980; Falk and Cohen, 1984) than for sheep Purkinje strands (Deitmer and Ellis, 1978; Eisner and Lederer, 1980; Eisner et al., 1981b; Glitsch et al., 1981; Glitsch and Pusch, 1984). Cohen et al. (1984) noticed that the larger values for kinetic estimates of $K_{0.5}$ obtained from sheep than from canine Purkinje strands is difficult to explain on the basis of saturability of the internal Na^+ site. This study suggests that differences in the reported values for $K_{0.5}$ could be accounted for by the well documented anatomical differences.

DiFrancesco and Noble (1985) using mathematical modeling techniques recently also examined the effects of interstitial K^+ depletion on the apparent $K_{0.5}$ of the Na^+ pump. The main emphasis of their comprehensive model simulating cardiac electrical activity was directed toward questions only peripherally related to K^+ -activated Na^+ pumping, and a detailed account of their analysis of the K^+ kinetics of the Na^+ -pump was not provided. A direct comparison between their study and this study is therefore difficult. Qualitatively their conclusions regarding the effect of K^+ depletion on $K_{0.5}$ are similar to those of this study. However, there are some critical differences in the behavior of the two models at low levels of $[\text{K}^+]_o$. Outward membrane current and a decline in $[\text{Na}^+]_i$ occurred on pump activation with a $[\text{K}^+]_o$ of 2–15 mM in the example DiFrancesco and Noble used to illustrate effects of interstitial K^+ depletion (Fig. 15), but no outward current developed and $[\text{Na}^+]_i$ remained at a high level (25 mM) on pump activation with a $[\text{K}^+]_o$ of 1 mM. In contrast, comparable simulations in this study produced outward pump currents and a fall in $[\text{Na}^+]_i$ when $[\text{K}^+]_o$ was 1 mM (see Figs. 4, 5, and 6), results that mimic published, experimentally obtained data (see Figs. 1 and 2, Eisner et al., 1981b). The reasons for the difference between the results of simulations at low $[\text{K}^+]_o$ using the model of DiFrancesco and Noble and those presented in this article are not apparent to us.

Depletion of pump-activating cations in narrow extracellular spaces has also been discussed as a possible source of error in estimating $K_{0.5}$ by others (Eisner and Lederer, 1980; Eisner et al., 1981b; Cohen et al., 1984). However, it was speculated that a linear relationship between $[\text{Na}^+]_i$ and pump current, a monoexponential decay of the cur-

rents, and independence of the rate constants for this decay of the Na^+ load and E_m can provide evidence against depletion being a major source of error. Serious doubt about this notion is raised by the simulations presented here, and it is suggested that the discrepancy between kinetic and steady state estimates of $K_{0.5}$ in sheep Purkinje strands can arise as a consequence of delays in achieving equilibration of K^+ in narrow extracellular clefts. Saturability of the internal Na^+ site may also contribute to errors in the analysis of the Na^+ -pump's K^+ dependence, as demonstrated by Cohen et al. (1984). However, while it is probable that the Na^+ site saturates at some level of $[\text{Na}^+]_i$, the present study suggests that the discrepancy between kinetic and steady state estimates of $K_{0.5}$ reported from experiments on sheep Purkinje strands should not be viewed as evidence for saturation occurring at the levels of $[\text{Na}^+]_i$ typically obtained experimentally.

For the model used in this study it was assumed that the relationship between $[\text{Na}^+]_i$ and Na^+ -pump activity is linear, an assumption based upon available experimental data. An apparently linear relationship between $[\text{Na}^+]_i$ and pump activity does not, however, necessarily imply that the Na^+ site is nonsaturable. If, for example, the site exhibits saturability according to a simple Michaelis-Menten model, the relationship between $[\text{Na}^+]_i$ and pump activity may be approximately linear over the range of $[\text{Na}^+]_i$ obtained experimentally if the dissociation constant in the model is sufficiently large (DiFrancesco and Noble, 1985). This range of apparent linearity is further extended for a cubic model (Brink, 1983). Experimental data at the levels of $[\text{Na}^+]_i$ typically obtained may therefore be adequately simulated by the model used in this study despite saturability of the Na^+ site. However, to describe a saturable process with known kinetics over a wider range of $[\text{Na}^+]_i$, our model should be modified with the appropriate equation.

The authors thank Amy L. Cigan for her skillful art work and Mathew E. TenEick for his assistance in running simulations.

Supported by a Grant-in-Aid from the Chicago Heart Association, United States Public Health Service Grant HL-27026, the Brinton Trust, the Reingold Estate, and by a travel grant from the National Heart Foundation of Australia.

Received for publication 7 November 1985 and in final form 15 July 1986.

REFERENCES

- Baumgarten, C. M., and G. Isenberg. 1977. Depletion and accumulation of potassium in the extracellular clefts of cardiac Purkinje fibers during voltage clamp hyperpolarization and depolarization. *Pfluegers Arch. Eur. J. Physiol.* 368:19–31.
- Brink, F., Jr. 1983. Linear range of Na^+ pump in sciatic nerve of frog. *Am. J. Physiol.* 244:C198–C204.
- Cohen, I., R. Falk, and G. Gintant. 1984. Saturation of the internal sodium site of the sodium pump can distort estimates of potassium affinity. *Biophys. J.* 46:719–727.
- Coulombe, A., and E. Coraboeuf. 1983. Simulation of potassium accumu-

- lation in clefts of Purkinje fibers: effect on membrane electrical activity. *J. Theor. Biol.* 104:211–229.
- Deitmer, J. W., and D. Ellis. 1978. The intracellular sodium activity of cardiac Purkinje fibres during inhibition and re-activation of the Na-K pump. *J. Physiol. (Lond.)*. 284:241–259.
- DiFrancesco, D., and D. Noble. 1985. A model of cardiac electrical activity incorporating ionic pumps and concentration changes. *Philos. Trans. R. Soc. Lond. B. Biol. Sci.* B307:353–398.
- Eisenberg, B. R., and I. S. Cohen. 1983. The ultrastructure of the cardiac Purkinje strand in the dog: a morphometric analysis. *Proc. R. Soc. Lond. B. Biol. Sci.* B217:191–213.
- Eisner, D. A., and W. J. Lederer. 1980. Characterization of the electrogenic sodium pump in cardiac Purkinje fibres. *J. Physiol. (Lond.)*. 303:441–474.
- Eisner, D. A., W. J. Lederer, and R. D. Vaughan-Jones. 1981a. The dependence of sodium pumping and tension on intracellular sodium activity in voltage-clamped sheep Purkinje fibres. *J. Physiol. (Lond.)*. 317:163–187.
- Eisner, D. A., W. J. Lederer, and R. D. Vaughan-Jones. 1981b. The effects of rubidium ions and membrane potential on the intracellular sodium activity of sheep Purkinje fibres. *J. Physiol. (Lond.)*. 317:189–205.
- Falk, R. T., and I. S. Cohen. 1984. Membrane current following activity in canine cardiac Purkinje fibers. *J. Gen. Physiol.* 83:771–799.
- Gadsby, D. C. 1980. Activation of electrogenic Na^+/K^+ exchange by extracellular K^+ in canine cardiac Purkinje fibres. *Proc. Natl. Acad. Sci. USA*. 77:4035–4039.
- Gadsby, D. C. 1984. The Na/K pump of cardiac cells. *Annu. Rev. Biophys. Bioeng.* 13:373–398.
- Gadsby, D. C., and P. F. Cranefield. 1979. Direct measurement of changes in sodium pump current in canine cardiac Purkinje fibers. *Proc. Natl. Acad. Sci. USA*. 76:1783–1787.
- Gerald, C. F. 1980. Numerical solution of ordinary differential equations. In *Applied Numerical Analysis*. C. F. Gerald, editor. Addison-Wesley Publishing Co., Reading, MA 250–303.
- Glitsch, H. G., W. Kampmann, and H. Pusch. 1981. Activation of active Na transport in sheep Purkinje fibres by external K or Rb ions. *Pfluegers Arch. Eur. J. Physiol.* 391:28–34.
- Glitsch, H. G., H. Pusch, Th. Schumacher, and F. Verdonck. 1982. An identification of the K activated Na pump current in sheep Purkinje fibres. *Pfluegers Arch. Eur. J. Physiol.* 394:256–263.
- Glitsch, H. G., and H. Pusch. 1984. On the temperature dependence of the Na pump in sheep Purkinje fibres. *Pfluegers Arch. Eur. J. Physiol.* 402:109–115.
- Hellam, D. C., and J. W. Studdt. 1974. A core-conductor model of the cardiac Purkinje fibre based on structural analysis. *J. Physiol. (Lond.)*. 243:637–660.
- Mobley, B. A., and E. Page. 1972. The surface area of sheep cardiac Purkinje fibres. *J. Physiol. (Lond.)*. 220:547–563.
- Schoenberg, M., and H. A. Fozzard. 1979. The influence of intercellular clefts on the electrical properties of sheep cardiac Purkinje fibers. *Biophys. J.* 25:217–234.
- Takahashi, Y., M. J. Rabins, and D. M. Auslander. 1970. Control and Dynamic Systems. Addison-Wesley Publishing Co., Reading, MA. Ch. 2:35–57.
- Whisler, J. W., and D. Johnston. 1978. Epileptogenesis: a model for the involvement of slow membrane events and extracellular potassium. *J. Theor. Biol.* 75:271–288.